Collision-induced superfluorescence

A. Kumarakrishnan and Siddharaj Chudasama

Department of Physics and Astronomy, York University Toronto, Ontario M3J 1P3, Canada

Xianming Han

Department of Physics, Butler University, Indianapolis, Indiana 46208

Received July 19, 2004; revised manuscript received December 14, 2004; accepted January 9, 2005

We have studied superfluorescence (SF) in Ca vapor evolving on the $3d4s^3D_J$-$4s4p^3P_{J-1}$ transitions at 1.9 μm by exciting the $4s^{21}S_0$-$4s4p^1P_1$ with a pulsed dye laser. SF is generated following population transfer by spin-changing collisions with an inert gas Ar from the $4s4p^1P_1$ and $3d4s^1D_2$ levels. We show for the first time to our knowledge that the time delay for SF evolution follows the $1/\sqrt{N}$ dependence expected for the case of uniform excitation of the vapor column by collisional transfer. Here, N is the number of participating atoms that was measured directly from the photon yield. The measured photon yield for the signal as a function of Ar pressure was found to be consistent with rate equations that simulate the buildup of populations in the ^3D_J levels based on known collisional rates. This suggests that collisional rates can be directly inferred on the basis of SF photon yields and the atomic level populations. The pulse shapes for SF show temporal oscillations that depend on two distinct factors. The first is the presence of a number of independently evolving regions in the gain medium, and the second is the presence of spatial modes. Temporal ringing is a well-known effect related to the exchange of energy between the atoms and the radiation field during pulse propagation. However, the temporal ringing observed in this experiment is far more pronounced than in previous SF experiments due to a particular choice of evolution parameters. This should make it feasible to compare our results with detailed numerical simulations that have been carried out previously.

OCIS codes: 020.0020, 270.0270, 020.1670, 020.2070, 190.5530, 270.6630.

1. INTRODUCTION

During the past three decades, there has been considerable interest[1–4] in storing energy in the electronic states of the alkaline earths with the goal of identifying transitions for laser emissions out of these levels. These electronic states have been produced as a by-product of chemical reactions[5–7] or as a result of direct collisional transfer of populations from the upper levels. Here, we describe our investigations of the properties of superfluorescence (SF) emission near 1.9 μm on the $3d4s^3D_J$ -$4s4p^3P_{J-1}$ transitions in Ca vapor as a result of spin-changing collisions with a perturbing gas (Ar). These collisions transfer populations to the ^3D_J levels from the $4s4p^1P_1$ and $3d4s^1D_2$ levels (see Fig. 1). In this case, the $4s4p^1P_1$ levels were excited by a pump laser tuned to the vicinity of the $4s^{21}S_0$-$4s4p^1P_1$ transition.

SF refers to the evolution of an initial population into a coherent state by means of coupling through a common electromagnetic field.[8–11] The process starts from spontaneous emission and results in a burst of radiation. The evolution of a SF pulse is influenced by quantum fluctuations so that the pulse amplitude, pulse width, and evolution time (or delay time, generally defined as the time between the onset of the excitation pulse and the peak of the SF pulse) show characteristic statistical variations from shot to shot. In this work, we have measured the delay time for the 1.9-μm SF transition by varying the ^3D_J population. Our results indicate that the delay time exhibits the predicted $1/\sqrt{N}$ dependence, where N is the number of participating atoms. This scaling law is related to the existence of a number of independently evolving slices in the sample and can be expected to apply to a variety of atomic systems that are transversely excited. Examples include atomic beams and SF-like lasers such as the Cu vapor laser,[12] which utilizes electron impact collisions for uniform excitation of the gain medium. However, perhaps somewhat surprisingly, to our knowledge this scaling law does not seem to have been observed in previous work. Another aspect of our studies is that we measure the delay time and the number of participating atoms directly from the photon yield. Previous SF experiments have relied on indirect estimates of the dipole coupling time to establish scaling laws.[13] Therefore our measurements of the scaling laws are also more precise compared with previous work.

We have studied the dependence of the photon yield for the 1.9-μm SF on Ar pressure and modeled the results using simple rate equations to describe the ^3D_J population. We use the most accurate measurements of relevant collisional rates[14] for this analysis. The measurements in Ref. 14 were based on laser-induced fluorescence experiments in which the time-dependent populations of excited levels were recorded. In these experiments, it was crucial to ensure that the effects of radiation trapping were neg-

0740-3224/05/071538-9/$15.00

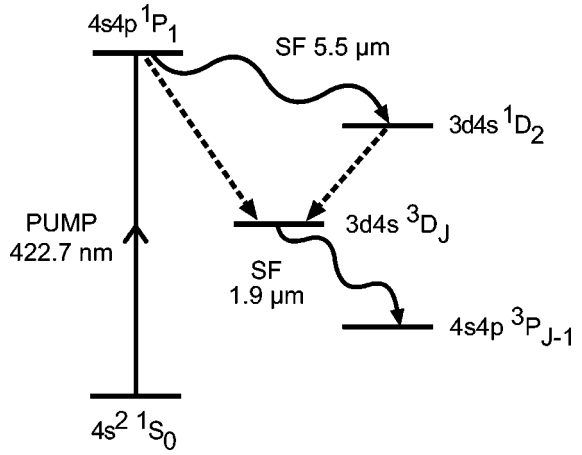

Fig. 1. Ca energy level diagram. Wavy lines show SF transitions; dashed lines show collisional channels; the solid line is the pump transition.

ligible. The agreement between our data and the simplified rate equation analysis suggests that it should be possible to infer the collisional rates by measuring the SF photon yields and improving the precision associated with our measurements of the excited level populations. An important distinction is that this technique would be immune to the effects of radiation trapping.

We also present for the first time to our knowledge convincing evidence for temporal oscillations in SF pulses that are attributed to absorption and reemission of radiation as the pulse propagates between independently evolving regions within the sample. Competition between spatial modes is also shown to reduce the temporal ringing. Temporal ringing in SF has been studied extensively on the basis of simulations,[11,15] and there is a general understanding of effects that contribute to the ringing observed in our experiments. However, the comparison between experiment and simulations[11] is strikingly inadequate. The temporal ringing observed in this work is very pronounced because the evolution parameters in the Ca system are clearly different from previous work. This makes it possible to make detailed comparisons between simulation and theory.

The rest of this paper is organized as follows. In Section 2 we review related work in Sr and Ca, the properties of the Ca atomic system, and measurements of collisional cross sections used for understanding the mechanism of population transfer to the ^3D_J levels. In this section we also introduce scaling laws that have been predicted for SF and discuss the origin of temporal ringing. In Section 3 we give a brief description of the experiment, and Section 4 contains a discussion of the results.

2. MECHANISM OF POPULATION TRANSFER

A. Properties of the Calcium Atomic System

It has been known that inelastic collisions are effective in transferring population from the $5s4p\,^1P_1$ and $5s4d\,^1D_2$ levels to the $5s4d\,^3D_J$ levels in Sr.[1] When the $^1S_0$-$^1P_1$ transition was excited with a 10-ns pulse from a dye laser (peak power of 300 kW) in the presence of a buffer gas (He at ~800 Torr), laser emissions near 6.5 μm on the $5s5p\,^1P_1$-$5s4d\,^1D_2$ transition and near 2.9 μm on the $5s4d\,^3D_J$-$5s5p\,^3P_{J-1}$ transitions were observed. The peak power of the latter emissions of ~4 kW was an order of magnitude larger than the peak power of the 6.5-μm emission. The ^3D_J levels were thought to be populated in two steps. The first step was considered to involve direct collisional transfer from the $^1P_1$ level to the metastable $^1D_2$ level. This was thought to result in the diminution of the intensity of the 6.5-μm emission. The second step was inferred to be a result of a spin-changing collision from $^1D_2$ to ^3D_J. It was also demonstrated that the rates for collisional transfer from $^1D_2$ to $^3P_{J-1}$ and from ^3D_J to $^3P_{J-1}$ were negligible.

Subsequent measurements of the overall cross sections for excitation from $^1P_1$ to ^3P_J were carried out in Sr and Ca.[16] The experimental conditions were designed to avoid cooperative emission on at least the $^1P_1$-$^1D_2$ transition. Once again, significant collisional depopulation of the $^1P_1$ level was observed.

Similar measurements were performed in Ca.[17] However, the pathways of population transfer to the ^3P_J levels were not identified. In this work it was assumed that the transfer occurred in a two-step process from the $^1P_1$ to the $^1D_2$ and then from $^1D_2$ to ^3D_J. The results suggested that the rate of transfer from $^1P_1$ to $^1D_2$ was at least a factor of 10 smaller than the rate for $^1D_2$-^3D_J.

The work of Ref. 18 showed conclusively that the assumption of a two-step process was not justified. The relative populations of the $^1D_2$ and ^3D_J levels in Ca were measured with a probe laser pulse applied ~8 ns after excitation of the $^1P_1$ level. In the absence of SF at 5.5 μm, an almost exclusive production of the ^3D_J levels was observed. The branching ratio for collisional deactivation of the $^1P_1$ state to the ^3D_J levels was over 0.9 for all noble gases. Furthermore, a nearly statistical mixture of populations (7:5:3) in the ^3D_J levels was observed even at Ar pressures of ~25 Torr.

Refined measurements have been reported in Ref. 14 for the absolute values of the rate coefficients for collisional deactivation of the $^1P_1$ and $^1D_2$ levels to the ^3D_J levels in Sr. Using values of $k_1(^1P_1$-$^3D_J)=2\times10^{-11}$ cm^3 s^{-1} and $k_2(^1D_2$-$^3D_J)=4.3\times10^{-11}$ cm^3 s^{-1} for Ar from Ref. 14, we estimate corresponding rate coefficients in Ca to be $k_1\sim5.7\times10^{-13}$ cm^3 s^{-1} and $k_2\sim1.2\times10^{-12}$ cm^3 s^{-1}. This estimate is based on the measurements of the total $^1P_1$-^3P_J cross sections that was found to be in the ratio of $\sigma(\mathrm{Sr})/\sigma(\mathrm{Ca})\sim35$.[16] Since the experiment described in this paper was carried out at a cell temperature of ~900 K, the values for the rates in Ref. 14 that were obtained at 750 K were corrected by a factor of 1.1 for the temperature difference (since the relative velocity scales as $\sqrt{T}$) and then by a factor of 35 to obtain the corresponding rates for Ca.

In this work, we find that the $^1P_1$ level can be populated in the presence of a small concentration of Ar gas (~1 Torr) even when the pump laser is detuned by several wave numbers. This process involves collisional transfer from the dressed states and multiphoton processes.[19] After the turnoff of the pump laser, a substantial fraction of the ground-state population (the typical $^1S_0$ density $\sim5\times10^{14}$ cm^{-3}) is present in the $^1P_1$ state.

Although the lifetime of the $^1P_1$ level is less than ~5 ns,[20] radiation trapping preserves the excited-state population for time scales of the order of ~1 μs, thereby allowing SF to evolve on the $4s4p\,^1P_1$-$3d4s\,^1D_2$ transition at 5.5 μm.[21] Although the radiative rate for the 5.5-μm transition is small (3.68×10^3 s^{-1}, as measured in Ref. 22), this process can occur with a quantum efficiency of order unity.[21] This SF emission has a characteristic delay time that can vary from ~10 to 50 ns. We also note that the lifetime of the metastable $^1D_2$ state is ~1 ms.[2] Therefore the ^3D_J levels can be excited by collisional transfer from the $^1P_1$ (starting immediately after the pump pulse) and the $^1D_2$ levels following the evolution of 5.5-μm SF. Subsequently, SF emission is observed to occur on the ^3D_J-$^3P_{J-1}$ transitions with delay times of ~30–100 ns. This delay time was always larger than the delay time for the 5.5-μm SF. As expected, the delay time for 1.9-μm SF is much shorter than the radiative decay time of the ^3D_J levels (~2.9 μs).[14] Increasing the Ar buffer gas pressure results in an increase in the SF photon yield of both 5.5- and 1.9-μm SF emissions until the collisional rate is sufficiently large to dephase the cooperative emission.[21] The radiative rate of the $^3P_{J-1}$ levels is ~400 μs (Ref. 23) and is known to have an effective decay time of ~1 ms due to intermultiplet transfer at high buffer gas pressure.[16] Thus the excited system relaxes to the ground state on a time scale of ~10 ms. This makes it possible to operate the pump laser at a rate of 10 Hz.

B. Superfluorescence Scaling Laws

SF has been studied extensively over the past few decades, and this work has been thoroughly reviewed in Refs. 9–11 and 24. Other applications of SF relating to new schemes for laser emissions are described in Refs. 25 and 26, and applications pertaining to free electron lasers are described in Ref. 27. There is continued interest in studying SF for improving theoretical understanding,[28] for detecting species concentrations,[29,30] for determining molecular level structure,[31] and in the context of generating new nonlinear effects.[32]

The scaling laws for SF can be quantified in terms of the propagation time τ_E for light through the medium and the dipole coupling time τ_R given by $\tau_R=1/N\Gamma\mu$.[24] Here N is the number of participating atoms, Γ is the radiative rate for the SF transition, and $\mu=(3/8\pi)(\lambda^2/A)$ is the diffraction solid angle of the cylindrical interaction volume ($\sim1.5\times10^{-7}$ for $\lambda=1.9$ μm). Here A is the area of cross section of the cylinder. The effect of μ is to amplify modes associated with the long axis of the cylindrical column. The threshold for SF occurs when $\tau_R=T_2$, where T_2 is the effective dephasing time that has contributions from natural broadening, Doppler broadening, and collisional dephasing.

For longitudinal or swept excitation, no upper limit on the number of atoms participating in SF is expected since SF, initiated in time τ_R, follows the pump pulse through the amplifying medium at nearly the same speed. For transverse excitation, as in pulsed excitation of an atomic beam, SF can evolve over a column of length L only if $\tau_E<\tau_R$. This yields an upper limit for the largest number of atoms N_c that can emit cooperatively.[33] The SF peak intensity $\propto N^2$ and the pulse width scales as $1/N\Gamma$. The SF delay time τ_D scales as $1/N$ in this regime. It is this regime that has been extensively explored in early SF experiments reviewed in Refs. 9–11 and 24. If $\tau_E>\tau_R$, the effects of propagation become important. The excited column can be considered to be divided into a number of noninteracting slices, each of which emits cooperatively.[24] In this regime, the SF peak intensity $\propto N$, the pulse width scales as $1/\sqrt{N}\Gamma$, and the delay time that is proportional to the dipole coupling time $\tau_{R'}$ of a single slice is $\propto1/\sqrt{N}$.

Our experiments were specifically designed to observe this scaling law since it can be expected that the buildup of ^3D_J states will be uniform along the length of the cell and result in a $1/\sqrt{N}$ dependence for τ_D. Another feature of collisionally induced SF is that the emission can be insensitive to any coherent effects created by the pump pulse.[34,35] Such effects can appreciably change the scaling laws describing the properties of SF pulses.

It should be noted that the atomic beam experiment in Ref. 13 was operated mostly in the regime of pure SF. Although the regime characterized by $\tau_E>\tau_R$ could be accessed in these experiments, no measurements of the delay time were reported in this regime. However, changes in the SF pulse shapes were observed under conditions for which $\tau_E=\tau_R$.

C. Temporal Ringing

The Fresnel number of the system given by $F=A/\lambda L$ can be used to characterize the shape of the volume of the excited column. This parameter specifies the modes of the radiation field to which the dipoles are coupled, since F^2 is a measure of the number of spatial modes.[36] When $F>1$, the geometric solid angle of the excited atoms is larger than the diffraction angle of a mode, and consequently a large number of modes can contribute to the emission. When $F<1$, only a single mode can contribute. But this mode has a large divergence that results in attenuation of the SF pulse due to diffraction.

To a good approximation, the variation in the electric field evolving along the long axis of the cylindrical column can be limited to being only along the propagation direction if F is of the order of unity. However, this is true only if $\tau_E<\tau_R$. If $\tau_E>\tau_R$, the division of the sample into a number of slices implies that $F>1$ for each slice if $F=1$ for the entire column.

The evolution of SF has been described both by semiclassical mean-field theories[37–40] and by fully quantum-mechanical theories,[41,42,24] which account for the effects of pulse propagation. Both theories predict temporal ringing in the SF pulses by solution of the Maxwell–Bloch equations. Although the mean-field theory regards all atoms as being subject to the same local environments (all atoms evolve because of the same noise term), the quantum-mechanical theories divide the atoms into many regions within which all atoms have the same noise term. Thus atoms in the sample evolve in differing local environments. The mean-field theory also ignores the fact that, during the classical stage of emission (a few τ_R into the evolution), the values of the atomic polarization, electric field, and number density acquire different values in different regions of the sample within a single slice. The propagation theories take this into account.

As a result, the mean-field theory predicts smooth sech^2 pulses corresponding to an overdamped Bloch vector swinging smoothly between the excited state and the final state. It does, however, predict fluctuations in the time delay from shot to shot.[24]

The quantum-mechanical theories, on the other hand, predict temporal ringing even for the case of a single slice. Since the atoms in different regions evolve at different rates, there is an exchange of energy between the atoms and the evolving field resulting in oscillations of the Bloch vector as it settles into its position in the final state. The quantum-mechanical theories also predict shot-to-shot fluctuations in time delay, peak height, temporal ringing, and pulse shapes.[24]

As the number of independent slices increases, the mean-field theory also predicts oscillations for the Bloch vector. The temporal ringing is caused by absorption and reemission of radiation during the propagation. The SF pulse shape is thus a succession of sech^2 pulses of diminishing intensity.

In the presence of dephasing, the length of the Bloch vector shortens as it reaches the final position, and the energy transferred to the adjacent slice is reduced. This causes the temporal ringing to be damped. It has been shown in Refs. 43 and 44 that the mean-field theory, in the absence of dephasing, predicts that the number of temporal lobes will be equal to the number of slices.

The predictions made by the quantum-mechanical treatment are very similar to those of the mean-field theories when a number of slices are present in a sample. The ringing produced by a single slice will rapidly get smeared out when the radiation passes from one slice to the other. For a large number of slices, the output will show ringing only because of absorption and reemission during propagation. Once again, in the presence of dephasing, the ringing can be expected to be damped.

Among several reports of SF experiments, three are noteworthy for their attempts to understand the origin of the ringing. The experiments of Ref. 45 in hydrogen fluoride gas were performed with a single slice and showed less ringing than predicted by Ref. 46. This was attributed to diffraction losses, although the experiment was performed with a Fresnel number close to one. However, the results were interpreted in Refs. 43 and 44 to be in accord with the ringing predicted by quantum-mechanical theories.

An experiment in a Cs atomic beam[13] yielded smooth pulses when the number of slices was of the order of unity and pulses with oscillations when the number of slices was increased. It was shown in Refs. 43 and 44 that such behavior was in reasonable agreement with the predictions of the mean-field theory.

In Ref. 47 a single velocity group of excited atoms was prepared in a Rb cell, and the experiment was performed in the single-slice regime. Temporal ringing was observed when a pinhole was placed at the center of the SF beam. The ringing was washed out because of spatial averaging without the pinhole. These results showed that the ringing was intrinsic to SF and suggested that the Cs experiment saw smooth pulses in the single-slice regime because of spatial averaging. It is believed that the small amount of ringing in the hydrogen fluoride gas experiment was on account of the detector subtending most of the pulse. These conclusions on the effect of spatial averaging are in accord with the results of Ref. 15. In this work, transverse effects in SF were studied through extensive numerical simulations. The results show that, for a Fresnel number of the order of unity, the active area of the detector would have to be much smaller than the SF beam size to observe ringing in the single-slice regime. Other effects that can reduce temporal ringing relate to interference between forward- and backward-going SF pulses.[48] The influence of radiation trapping in reducing the temporal ringing of 5.5-μm SF was considered in Ref. 49.

3. EXPERIMENTAL DETAILS

The experiment was carried out in a stainless-steel cell of length 50 cm. Ca pellets were loaded in the region between knife-edge baffles at either end of the cell. The temperature of the cell ($\sim$900 K) was uniform and could be controlled to within $\pm 2^\circ$C. The pressure of the Ar gas (research purity $>$ 99.9995%) was measured by a capacitance manometer calibrated to $\pm$0.2%.

The Ca column was longitudinally pumped by pulses from a multimode (1–2-GHz bandwidth) homemade dye laser tuned to the vicinity of the principal resonance line at 4227 Å (see Fig. 2). The dye laser was pumped by light from a frequency-tripled (355-nm) commercial YAG laser that has a repetition rate of 10 Hz. The dye laser consisted of a double-grating oscillator cavity (Littman design), which was transversely pumped, and three amplifying stages. The pump pulse had a FWHM of 6 ns and an average energy per pulse of $\sim$1.5 mJ as measured with a calibrated thermopile ($\pm$2%). The spatial profile of the pump laser was Gaussian. The beam was collimated to have a confocal parameter greater than the length of the cell.

The IR emissions from the cell were incident on a Ge:Hg detector that had a home-built transmission line. The crystal was mounted on a cryorefrigerator operating on compressed He and cooled to $\sim$30 K. The bandwidth of the detector was assessed to be $\sim$350 MHz.

While studying the temporal features of SF, we made sure to arrange the Ge:Hg detector so that the diffraction angle of the IR was much greater than the subtended solid angle of the detector.

The output of this detector was connected either directly to a 1-GS/s digitizing oscilloscope with a suitable amplifier. The scope was triggered by the pump pulse incident on a Si p-i-n photodiode that had a rise time of

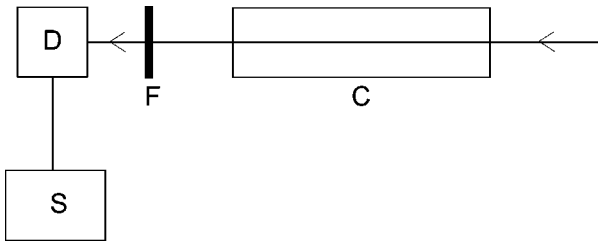

Fig. 2. Schematic of experiment. C, cell with Ca and Ar; D, detector; S, oscilloscope; F, filter or spectrometer.

<1 ns. The area under the pump pulse was held constant to within ~10% during the entire experiment.

The SF emissions at 5.5 and 1.9 μm could be spectrally resolved with suitable IR bandpass filters, or a 0.75-m monochromator (with a 75 grooves/mm grating blazed for 10 μm).

The ground-state density was measured with an uncertainty of ±30% by attenuating the pump laser, scanning it across the $4s^2 {}^1S_0$-$4s4p {}^1P_1$ transition, and measuring the integrated linewidth.[50] The same technique was used to infer the $^1P_1$ immediately after the pump pulse.[21] The absolute yield of SF photons was measured with a $LiTaO_3$ pyroelectric detector calibrated (±15%) against the thermopile. This detector and its home-built amplifier had ~1-nJ energy resolution at a signal-to-noise ratio of order unity. The number of photons in the SF pulse was approximately the same for emissions from the back and front ends of the cell. The total SF photon yield is used in the analysis of the data.

Of the six possible SF transitions to the ^3P levels, three ($^3D_3$-$^3P_2$, $^3D_2$-$^3P_1$, and $^3D_1$-$^3P_0$) have been found to occur in Sr.[1,3] These correspond to the three largest transition probabilities. We were able to observe only the $^3D_3$-$^3P_2$(1.97-μm) and $^3D_2$-$^3P_1$(1.95-μm) emissions in Ca after spectrally separating the components. This behavior is consistent with the findings in Ref. 14 that suggest that the population distributions in the ^3D_J state were not statistical and favored the strongest transitions.

4. RESULTS AND DISCUSSION

A. Time Delays

Figure 3 shows the observed time delays (measured from the 10% point at the leading edge of the pump pulse to the peak of the SF pulse) as a function of the SF photon yield N. The data were obtained at an Ar pressure of 405 Torr. The only SF emission present was due to the 1.97-μm transition. The number of participating SF atoms (SF photon yield) was measured by varying the pump laser detuning. The dashed line is the delay time predicted by

$$T_D = \tau_R \left[\frac{1}{4} \ln(2\pi N) \right]^2, \tag{1}$$

with N replaced by the number of atoms N' in each slice and τ_R replaced by the dipole coupling time of a single slice $\tau_{R'}$. Here, the number of atoms in each slice N' was estimated from $S = N/N' = \sqrt{\tau_E/\tau_R}$. Equation (1) was derived from a fully quantum-mechanical description.[41] This line exhibits $\sim 1/\sqrt{N}$ power-law dependence discussed earlier. Thus the data seem to be consistent with the dependence predicted for the case of a number of independent slices in the excited column. The $1/N$ dependence predicted by Eq. (1) is shown in Fig. 3 as the dotted line, and it clearly does not model the data.

We now discuss reasons that can contribute to the discrepancy between the dashed line and the data. The first relates to the uncertainty in the knowledge of the time at which the ^3D_J population is sufficiently large so that $\tau_{R'} < T_2$ and SF begins to evolve. Fitting the data to the form $1/N^x + b$ gives $x = 0.37 \pm 0.050$ and a temporal offset $b = 9.4$ ns (solid line). The value of the offset suggests that the ^3D_J begins evolving collectively at the end of the pump pulse. The second factor relates to the relatively small correction that has to be applied to the theoretical expression for the time delay to account for the effect of dephasing. Such a correction would affect the predicted values for smaller N more than it would for larger N. Another reason could include the presence of multiple spatial modes. Intramultiplet mixing, which shuffles populations within the ^3D_J states [6×10^7 (s/atom) at 400 Torr], is also expected to have a small contribution.

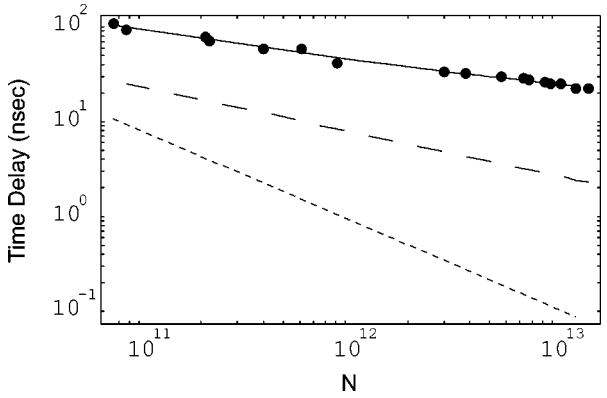

Fig. 3. Time delay of 1.9-μm SF measured from the beginning of the pump pulse versus SF photon yield N. Ar pressure is 405 Torr; pump beam diameter is 0.19 cm; $[^1S_0] = 3.9 \times 10^{14}$; circles represent the data; dashed line is $1/\sqrt{N}$ predicted by Eq. (1) with N replaced by N'; dotted line is $1/N$ dependence predicted by Eq. (1); solid line is the power law fit to the data by $a/N^x + b$, which gives $x = 0.37 \pm 0.050$ and $b = 9.4 \pm 5.0$ ns.

B. Photon Yields

The data in Fig. 4(a) show the photon yield at 1.9 μm due to all observed SF emissions as a function of Ar pressure. Figure 4(b) shows a comparison of the photon yields for 5.5 and 1.9-μm SF as a function of Ar pressure.

The pump laser power is ~100 kW. The diameter of the collimated pump beam corresponded to a Fresnel number $F = 2.9$ for the 1.9-μm SF as calculated for the entire column. Spectrally resolving the SF shows that the $^3D_3$-$^3P_2$ emission at 1.97 μm was dominant and that it peaks at ~700 Torr. The peak intensity of the $^3D_2$-$^3P_1$ emission at 1.95 μm occurred at ~150 Torr but it was approximately ten times smaller than the peak intensity of the 1.97-μm emission. Thus the intensities of both emissions initially increase with increasing buffer pressure until the collisional rate becomes large enough to dephase the SF. No SF was observed on the four other possible transitions. Similarly, the peak intensity for the 5.5-μm SF emission occurs at ~300 Torr, and this emission was collisionally dephased at a pressure of ~800 Torr.

The solid curve in Fig. 4(a) shows the population of the ^3D_J levels based on a rate equation model. The model assumes that the buildup of these population $N_{^3D_J}$ in ^3D_J levels can be written as a system of differential equations expressed as

$$\frac{dN_{^1P_1}}{dt} = -\Gamma_{T_{P-D}} N_{^1P_1}, \tag{2a}$$

$$\frac{dN_{^1D_2}}{dt} = -\Gamma_{T_{D-D}} N_{^1D_2}, \tag{2b}$$

$$\frac{dN_{^3D_J}}{dt} = \Gamma_{T_{P-D}} N_{^1P_1} + \Gamma_{T_{D-D}} N_{^1D_2}. \tag{2c}$$

Here, $N_{^1P_1}$, $N_{^1D_2}$, and $N_{^3D_J}$ are level populations. $\Gamma_{T_{P-D}}$ and $\Gamma_{T_{D-D}}$ are the total collisional loss rates out of $^1P_1$ and $^1D_2$, respectively. We assume that the collisional rate depends on the buffer gas pressure as described by $\Gamma = n_{\mathrm{Ar}} \sigma v$. Here, n_{Ar} is the density of Ar, σ is the collisional cross section, and v is the relative velocity of colliding atoms. As discussed in subsection 2.A, the above system of equations was solved assuming temperature-corrected collisional rates based on measured values for the Sr–Ar system[14] and the relative values of the Sr–Ca rates reported in Ref. 16.

We made several assumptions to simplify the analysis. We neglected the radiative rate for the $^1P_1$ level. This is because radiation trapping preserves the $^1P_1$ excitation for time scales of ~ 1 μs, which is much larger than the delay times for the 5.5- and 1.9-μm SF emissions. We also neglected the radiative decay of the $^1D_2$ and ^3D_J states since the corresponding lifetimes are much larger than the SF time delays.

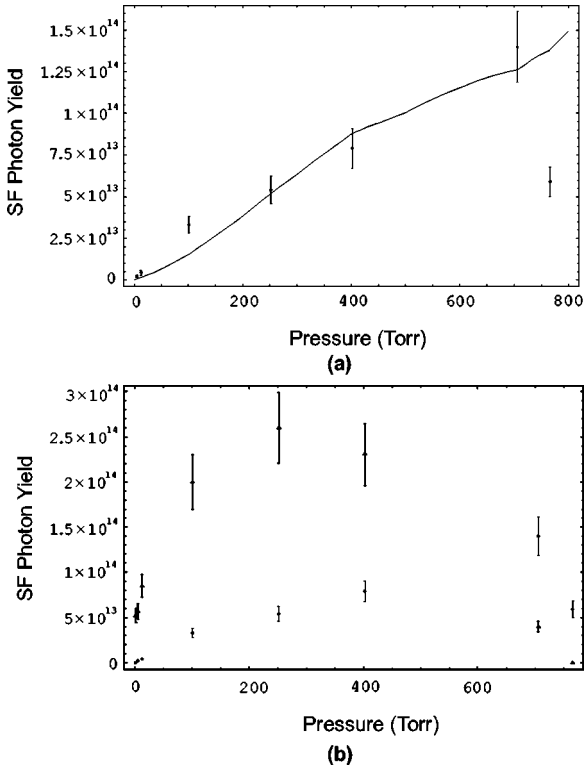

Fig. 4. (a) Photon yield of 1.9-μm SF as a function of Ar pressure. Dots represent the data; solid curve is the result of the model discussed in the text for the population of the ^3D_J level. There was no scaling to match the photon yield with the calculated population. The drop in SF photon yield above 700 Torr is attributed to collisional dephasing, an effect that is ignored by the model. (b) Absolute photon yields for 5.5-μm (triangles) and 1.9-μm (circles) SF emissions as a function of Ar pressure. In both (a) and (b) the error in the measured photon yields is ±15%.

Although the population transfer to the ^3D_J levels can be modeled on the basis of rate equations, the dynamics can be quite complicated, given the gas kinetic rates for collisional mixing between the ^3D_J fine-structure levels ($\sim 5\times10^{-10}$ cm^3 s^{-1} in Sr according to Ref. 14 and estimated to be $\sim 1.4\times10^{-11}$ cm^3 s^{-1} in Ca based on the measurements of Ref. 16). We therefore chose to ignore this effect. Similarly, the collisional rates for intramultiplet mixing between $^3P_{J-1}$ levels, which can be of the order of 10^{-10} cm^3 s^{-1} and result in population transfer during the time scale of SF emission, were ignored.[51] We also ignore the collisional transfer from $^1P_1$ to $^1D_2$ since the corresponding collisional rate is known to be considerably smaller than the collisional rate from $^1P_1$ to ^3D_J.[14] Thus the ^3D_J level is populated mainly by collisional transfer from the $^1D_2$ and $^1P_1$ levels.

We note that the $^1P_1$ level is populated by collisional transfer from the dressed states in the presence of the pump laser and by multiphoton processes during the pump pulse.[21,19] As a result, the $^1P_1$ population is known to increase as a function of Ar pressure. For this reason, the intensity of the 5.5-μm SF emission initially increases with Ar pressure up to $\sim$300 Torr until collisional dephasing gradually destroys the signal at pressures of $\sim$800 Torr.[21] Over this range of Ar pressures, the SF is known to occur with high efficiency and to transfer a variable fraction f_1 atoms from the $^1P_1$ to the $^1D_2$ level. As described in Ref. 21, the fraction was ~ 1 for an Ar pressure of 1 Torr. For higher pressures, the fraction was reduced and varied smoothly between 1 and 0.1 over the range of Ar pressures. f_1 was inferred from measurements of the $^1P_1$ population immediately after the pump pulse and from the measured 5.5-μm SF photon yield for a fixed Ar pressure. For this reason, we assume that the fraction of atoms that have not been transferred by SF out of the $^1P_1$ level are collisionally transferred to the ^3D_J levels.

We also assume that the population of the $^1D_2$ level at $t = \tau_{\mathrm{SF}}$ is given by the photon yield for 5.5-μm SF. Here, τ_{SF} is the delay time for 5.5-μm SF measured from the end of the pump pulse. We assume that these atoms are then collisionally transferred from the $^1D_2$ level to the ^3D_J level. For these reasons, it is possible to solve Eqs. (2) without a loss term for depopulation due to SF in Eq. (2a) and a corresponding buildup term in Eq. (2b).

In summary, we assume that the $N_{^1P_1}$ decays exponentially [as given by Eqs. (2)] as a function of time from its initial value at the end of the pump pulse due to the effect of collisions until the 5.5-μm SF pulse abruptly lowers the population at $t = \tau_{\mathrm{SF}}$. We assume that the $^1D_2$ state is populated instantaneously at this time and that it can then begin to collisionally populate the ^3D_J level. After the delay time τ_{SF}, atoms remaining in the $^1P_1$ level can also be transferred to the ^3D_J level by collisions. We assume that atoms remaining in $^1P_1$ and the atoms transferred into $^1D_2$ can then be collisionally excited into the ^3D_J until delay time τ_C, at which time the 1.9-μm SF is expected to evolve. We then calculate the ^3D_J population as a function of Ar pressure, assuming the values of τ_{SF} and τ_C measured in the experiment as well as the measured values of the $^1P_1$ population and the fraction f_1.

With these assumptions, the ^3D_J level population can

be obtained as a function of Ar pressure by writing the solution to Eqs. (2) in the following manner:

$$N_{^3D_J} = \Gamma_{T_{P-D}}\left(\int_0^{\tau_{SF}} N_{^1P_1}\mathrm{d}t + \int_{\tau_{SF}}^{\tau_C} N_{^1P_1}\mathrm{d}t\right) + \Gamma_{T_{D-D}}\int_{\tau_{SF}}^{\tau_C} N_{^1D_2}\mathrm{d}t. \quad (3)$$

The solid curve in Fig. 4 is the solution, assuming that the collision time τ_C extends over ~40 ns past the delay time of the 1.9-μm SF. This would imply that collisions transfer population for a time scale of the order of the duration of the 1.9-μm SF pulse (~100 ns). The solid curve is in reasonable agreement with the measured SF photon yield, suggesting that the ^3D_J level is being pumped during the evolution of SF. The disagreement at low Ar pressure is attributed to the sudden threshold for the onset of 1.9-μm transmissions.

The model agrees with the data if the collisional rates are varied within the ±25% error bars reported in Ref. 14. But the results predicted by the model do not agree with the data if the measured value of the $^1P_1$ population is varied by the extent of the error (±35%). In summary, the model seems to be consistent with experimentally measured parameters but is not sufficiently accurate to constitute a test of the collisional rates reported in Ref. 14 because of the error in the population measurements.

However, with the development of diode lasers, it has become possible to reduce the errors associated with the measurement of the $^1P_1$ population. This should make it possible to directly infer the collisional rates by measuring the 5.5- and 1.9-μm SF photon yields and the fraction of atoms in the $^1P_1$ level.

It is also necessary to develop a suitable model to describe the rapid collisional dephasing of 1.9-μm SF that is observed for Ar pressures >700 Torr. As in Ref. 21, we estimated the dephasing time for SF at 1.9 μm to be ~1.5 MHz Torr. We obtained this estimate using the results of Ref. 52 and by measuring the SF delay time at the perturber pressure (~800 Torr) for which the signal reverts to amplified spontaneous emission.

C. Temporal Ringing

Figure 5(a) shows the pulse shape of the 1.9-μm SF as a function of N for a fixed pump beam diameter and an Ar pressure of 766 Torr. Here, N was varied by adjusting the pump laser detuning. The number of slices was inferred based on the measured photon yield. The signal shows pronounced temporal ringing and that this ringing is preserved even for the time-averaged traces. When the pump laser detuning is varied, the number of participating atoms is reduced, causing in turn a smaller number of independent cooperative slices in the sample. As expected, the delay times are found to increase and the temporal ringing is reduced as shown in Fig. 5. The reduction in ringing is attributed in this case to the role of collisional dephasing during the increased evolution time. This effect broadens and smooths out the temporal oscillations. The data also qualitatively confirm the predictions of Ref. 53 in the regime where the sample contains several independent slices.

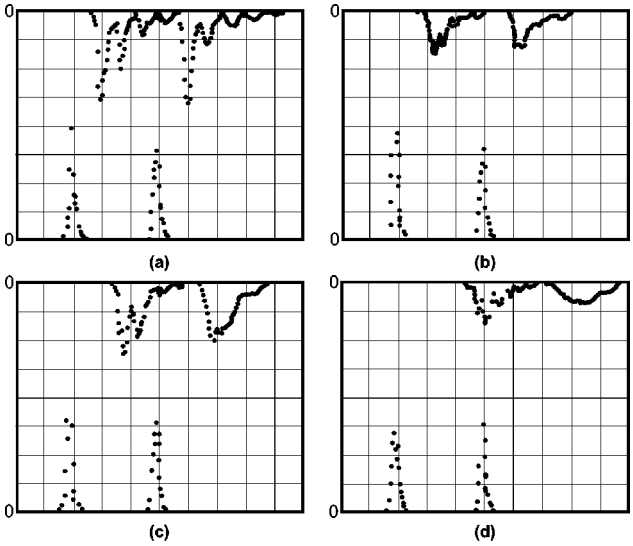

Fig. 5. Oscilloscope traces showing 1.97-μm SF pulses for four different photon yields N. Ar pressure is 766 Torr; pump beam diameter is 0.19 cm; horizontal time base is 25 ns division. Pump pulses are positive going and SF pulses are negative going because of bias voltages of respective detectors. Two records are overlayed in each graph; the first shows the pump pulse and corresponding SF pulse for a single shot; the second shows the average values of the pump and SF pulses obtained by averaging 256 repetitions. Zeros for SF and pump pulses are shown at the top and bottom of the graphs, respectively. (a) $N=5.9\times10^{13}$, $S=73$; (b) $N=2.2\times10^{13}$, $S=45$; (c) $N=7.2\times10^{12}$, $S=25$; (d) $N=4.6\times10^{12}$, $S=20$.

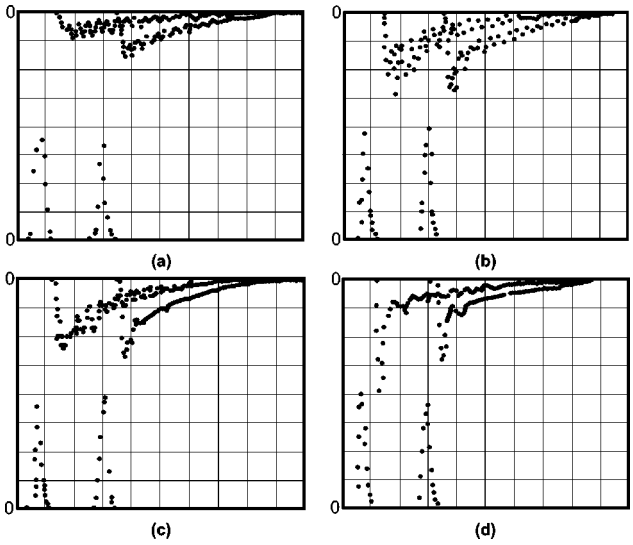

Fig. 6. Oscilloscope traces showing 1.9-μm SF pulses for four different pump beam diameters D. Ar pressure is 405 Torr; horizontal time base is 25 ns/division; vertical scale for SF pulses are 10 mV/division for (a) and (b), 20 mV/division for (c), and 100 mV/division for (d), Pump pulses are positive going and SF pulses are negative going because of bias voltages of the respective detectors. Two records are overlayed in each graph: the first shows the pump pulse and corresponding SF pulse for a single shot; the second shows the average values of the pump and SF pulses obtained by averaging 256 repetitions. Zeros for SF and pump pulses are shown at the top and bottom of the graphs, respectively. (a) $D=0.064$ cm, (b) $D=0.076$ cm, (c) $D=0.19$ cm, (d) $D=0.38$ cm.

We note that the ringing associated with the 5.5-μm emission[21] was very small in comparison. The essential differences between these two SF emissions seem to be that the radiative rate of the upper level was ≈650 times larger for the 5.5-μm emission. But the radiative rate for the 5.5-μm transition was ≈94 times smaller than the rate for the 1.9-μm SF transition. In addition, for the 5.5-μm SF, radiation trapping at the pump wavelength can cause atoms to be reshuffled into the velocity class (of the order of the natural linewidth) that participates directly in SF. This effect is negligible at 1.9 μm. Since the collisional dephasing rates for the two transitions are similar (~1 MHz/Torr), the temporal ringing observed for the 1.9-μm SF is attributed to the smaller dipole coupling time and the smaller effect due to radiative dephasing for this transition.

It can also be shown that the temporal ringing for the 1.9-μm SF depends on changes in the Fresnel number that can be effected by changing the pump beam diameter. Figure 6 shows the pulse shape as a function of increasing pump beam diameter at a fixed pump laser detuning and buffer gas pressure (405 Torr). At this pressure, there was only one contribution to the emission, namely, SF at 1.97 μm on the $^3D_3$-$^3P_2$ transition. The data show that the number of temporal lobes increases with an increase in the Fresnel number and that the ringing is washed out on averaging for larger Fresnel numbers. Distinct pulse shapes with varying numbers of temporal lobes were also obtained by imaging different radial sections of the SF pulse on the detector. Thus the data illustrate the effect of different spatial modes on the pulse shape.

5. CONCLUSIONS

Although many experiments have studied temporal ringing, our work offers the clearest evidence for ringing due to the propagation of the amplified radiation as it passes between independently evolving slices as well as the presence of spatial modes. The extent of ringing is attributed to a particular set of evolution parameters that are characteristic of the Ca atomic system. Since the SF evolution is decoupled from the coherent effects of the pump pulse, the data could be the basis to test detailed simulations that have been developed earlier.

The inversion between the ^3D_J and $^3P_{J-1}$ levels is regarded as being created uniformly along the length of the column. In this respect, the system seems to behave like a transversely excited system, and as a result the time delays show the predicted $1/\sqrt{N}$ dependence. Although SF has been widely studied, experiments have not tested predictions for scaling laws for SF delay times for the case of simultaneous excitation of the atomic column. This situation is encountered in atomic beams and laser amplifiers excited by collisions or electron impact. To the best of our knowledge, this work is the first confirmation of the $N^{-0.5}$ dependence of the delay time. In Ref. 21 this scaling law was observed for the case of swept excitation for entirely different reasons.

Finally, we note that the accuracy associated with the populations of the excited states can be improved considerably by use of diode lasers. This makes it feasible to infer collisional rates based on the photon yields for SF and the exited-state populations.

ACKNOWLEDGMENTS

These experiments were carried out at the University of Idaho in Jim Kelly's laboratory. The experimental work was supported by the National Science Foundation (NSF) Presidential Young Investigator Award, the NSF Experimental Program to Stimulate Competitive Research (Idaho), and the U. S. Air Force Weapons Laboratory. Subsequent analysis was supported by the Natural Sciences and Engineering Research Council (Canada), Canada Foundation for Innovation, Ontario Innovation Trust, Photonics Research Ontario, and York University.

REFERENCES

1. P. P. Sorokin and J. R. Lankard, "Infrared laser action in Sr vapor resulting from optical pumping and inelastic collisions," Phys. Rev. **186**, 342–343 (1969).
2. R. N. Diffenderfer, P. J. Dagdigian, and D. R. Yarkony, "Spin-forbidden radiative transitions in atomic Ca," J. Phys. B **14**, 21–27 (1981).
3. J. F. Kelly, M. Harris, J. Cooper, and A. Gallagher, "Competition of stimulated Raman and collision-induced stimulated emission in Sr," AIP Conf. Proc. **205**, 87 (1989).
4. A. Kumarakrishnan and X. L. Han, "Investigations of superfluorescent cascades," Opt. Commun. **109**, 348–360 (1994).
5. C. R. Jones and H. P. Broida, "Gas-phase reaction of Ba with N_2O. I. Measurement of production efficiency of excited states," J. Chem. Phys. **60**, 4369–4376 (1974).
6. D. J. Benard and W. D. Slater, "Mechanism of chemiluminescent chain reactions in Mg catalyzed N_2O–CO flames," J. Chem. Phys. **66**, 1017–1020 (1977).
7. B. E. Wilcomb and P. J. Dagdigian, "Visible chemiluminescence from the reaction of metastable Sr with N_2O: absolute cross section and photon yield," J. Chem. Phys. **69**, 1779–1781 (1978).
8. R. Bonifacio and L. A. Lugiato, "Cooperative radiation processes in two-level systems: superfluorescence," Phys. Rev. A **11**, 1507–1521 (1975).
9. A. V. Andreev, V. I. Emelyanov, and Yu. A. IIinskii, "Collective spontaneous emissions (Dicke superradiance)," Sov. Phys. Usp. **23**, 493–514 (1980).
10. M. F. H. Schuurmans, Q. H. F. Vrehen, D. Polder, and H. M. Gibbs, "Superfluorescence," in *Advances in Atomic and Molecular Physics*, D. Bates and B. Bederson, eds. (Academic, New York, 1981), pp. 167–228.
11. Q. H. F. Vrehen and H. M. Gibbs, "Superfluorescence experiments," in *Dissipative Systems in Quantum Optics*, R. Bonifacio, ed. (Springer-Verlag, Berlin, 1982), pp. 111–147.
12. T. W. Karras, R. S. Anderson, B. G. Bricks, and C. E. Anderson, "Visible cooperative emission in incoherently excited copper vapor," in *Cooperative Effects in Matter and Radiation*, C. M. Bowden, D. W. Howgate, and H. R. Robl, eds. (Plenum, New York, 1977), pp. 101–113.
13. H. M. Gibbs, Q. H. F. Vrehen, and H. M. J. Hikspoors, "Single-pulse superfluorescence in cesium," Phys. Rev. Lett. **39**, 547–550 (1977).
14. D. A. Miller, L. You, J. Cooper, and A. Gallagher, "Collisional energy transfer between excited-state strontium and noble-gas atoms," Phys. Rev. A **46**, 1303–1309 (1992).
15. F. P. Mattar, H. M. Gibbs, S. L. McCall, and M. S. Feld, "Transverse effects in superfluorescence," Phys. Rev. Lett. **46**, 1123–1126 (1981).
16. J. J. Wright and L. C. Balling, "$^1P_1 \rightarrow {}^3P_1$ excitation

transfer for Ca and Sr with the noble gases," J. Chem. Phys. **73**, 1617–1619 (1980).
17. M. Harris, D. R. McHugh, E. L. Lewis, I. Shannon, and M. Zokai, "Saturation of the calcium singlet resonance line and excitation transfer by collisions with rare gases," J. Phys. B **20**, 5575–5583 (1987).
18. W. H. Breckenridge and C. N. Merrow, "Nascent state distributions of $Ca(4s3d\,^1D_2)$, $Ca(4s3d\,^3D_J)$, and $Ca(4s4p\,^3P_J)$ in the collisional deactivation of $Ca(4s4p\,^1P_1)$ by the rare gases," J. Chem. Phys. **88**, 2320–2328 (1988).
19. A. Kumarakrishnan, S. Chudasama, and X. L. Han, "Superfluorescence polarization: signature of collisional redistribution," Phys. Rev. A **68**, 033801 (2003).
20. W. L. Wiese, M. W. Smith, and B. M. Miles, *Atomic Transition Probabilities*, Natl. Bur. Stand. (U.S.) Circ. No. 22 (U.S. GPO, Washington, DC, 1969).
21. A. Kumarakrishnan and X. L. Han, "Superfluorescence from optically trapped calcium atoms," Phys. Rev. A **58**, 4153–4162 (1998).
22. L. P. Lellouch and L. R. Hunter, "Measurement of the $4s4p\,^1P$-$4s3d\,^1D$ spontaneous emission rate in calcium by use of a Stark-electric-quadrupole interference," Phys. Rev. A **36**, 3490–3493 (1987).
23. P. S. Furcinitti, J. J. Wright, and L. C. Balling, "A measurement of the $^3P_1$ metastable state in Ca," Phys. Lett. **53**A, 75–76 (1975).
24. M. Gross and S. Haroche, "Superradiance: an essay on the theory of collective spontaneous emission," Phys. Rep. **93**, 301–396 (1982).
25. D. P. Scherrer and F. K. Kneubuhl, "New phenomena related to pulsed far-infrared superradiant and Raman emissions," Infrared Phys. **34**, 227–267 (1993).
26. P. D. Drummond, J. D. Harvey, J. M. Dudley, D. B. Hirst, and S. J. Carter, "Phase waves in mode-locked superfluorescent lasers," Phys. Rev. Lett. **78**, 836–839 (1997).
27. M. Hogan, C. Pellegrini, J. Rosenzweig, G. Travish, A. Varfolomeev, S. Anderson, K. Bishofberger, P. Frigola, A. Murokh, N. Osmanov, S. Reiche, and A. Tremaine, "Measurements of high gain and intensity fluctuations in a self-amplified, spontaneous-emission free-electron laser," Phys. Rev. Lett. **80**, 289292 (1998).
28. J. Meziane, S. Oullemine, K. Amezian, and E. Boursey, "Competition between collective and stimulated effects in $^{130}Te_2$ superluorescence," Chem. Phys. Lett. **363**, 573578 (2002).
29. A. D. Tserepi, E. Wurzberg, and T. A. Miller, "Two-photon-excited stimulated emission from atomic oxygen in rf plasmas: detection and estimation of its threshold," Chem. Phys. Lett. **265**, 297–302 (1997).
30. A. D. Tserepi and T. A. Miller, "Spatially and temporally resolved absolute O-atom concentrations in etching plasmas," J. Appl. Phys. **77**, 505–511 (1995).
31. E. Boursey, J. Meziane, and A. Topouzkhanian, "Superfluorescence beats in $^{125}Te_2$ emission," Phys. Rev. A **48**, 30473050 (1993).
32. A. I. Lvovsky, S. R. Hartmann, and F. Moshary, "Superfluorescence-stimulated photon echoes," Phys. Rev. Lett. **89**, 263602–263605 (2002).
33. F. T. Arecchi and E. Courtens, "Cooperative phenomena in resonant electromagnetic propagation," Phys. Rev. A **2**, 1730–1737 (1970).
34. C. M. Bowden and C. C. Sung, "Cooperative behavior among three-level systems: transient effects of coherent optical pumping," Phys. Rev. A **18**, 1558–1570 (1978).
35. C. M. Bowden and C. C. Sung, "Transient effects of dephasing and relaxation in cooperative evolution among three-level systems: II," Phys. Rev. A **20**, 2033–2039 (1979).
36. R. G. Wenzel, J. M. Telle, and J. L. Carlsten, "Fresnel diffraction in an optical system containing lenses," J. Opt. Soc. Am. A **3**, 838–842 (1986).
37. R. Bonifacio, P. Schwendimann, and F. Haake, "Quantum statistical theory of superradiance. I," Phys. Rev. A **4**, 302–313 (1971).
38. N. E. Rehler and J. H. Eberly, "Superradiance," Phys. Rev. A **3**, 1735–1751 (1971).
39. G. S. Agarwal, "Master-equation approach to spontaneous emission," Phys. Rev. A **2**, 2038–2046 (1970).
40. F. Haake, H. King, G. Schroder, J. Haus, and R. Glauber, "Fluctuations in superfluorescence," Phys. Rev. A **20**, 2047–2063 (1979).
41. D. Polder, M. F. H. Schuurmans, and Q. H. F. Vrehen, "Superfluorescence: quantum-mechanical derivation of Maxwell-Bloch description with fluctuating field source," Phys. Rev. A **19**, 1192–1203 (1979).
42. F. Haake, H. King, G. Schroder, J. Haus, R. Glauber, and F. Hopf, "Macroscopic quantum fluctuations in superfluorescence," Phys. Rev. Lett. **42**, 1740–1743 (1979).
43. R. Bonifacio, M. Gronchi, and L. A. Lugiato, "Superfluorescence: Maxwell–Bloch equations, mean-field approach, and Cs experiment," in *Coherence and Quantum Optics IV*, L. Mandel and E. Wolf, eds. (Plenum, New York, 1978), p. 939–951.
44. R. Bonifacio, M. Gronchi, L. A. Lugiato, and A. M. Ricca, in Ref. 12, p. 193.
45. N. Skribanowitz, J. P. Herman, J. C. MacGillivray, and M. S. Feld, "Observation of Dicke superradiance in optically pumped HF gas," Phys. Rev. Lett. **30**, 309–312 (1973).
46. J. C. MacGillivray and M. S. Feld, "Theory of superradiance in an extended, optically thick medium," Phys. Rev. A **14**, 1169–1189 (1976).
47. D. J. Heinzen, J. E. Thomas, and M. S. Feld, "Coherent ringing in superfluorescence," Phys. Rev. Lett. **54**, 677–680 (1985).
48. R. K. Bullough and R. Saunders, "Theory of FIR fluorescence", in *Cooperative Effects in Matter and Radiation*, M. Bowden, D. W. Hargate, and H. R. Robl, eds. (Plenum, 1977), pp. 209–256.
49. A. Kumarakrishnan, "An experimental investigation of superfluorescence in atomic calcium," Ph.D. dissertation (University of Idaho, Moscow, Idaho, 1992).
50. A. Corney, *Atomic and Laser Spectroscopy* (Oxford, New York, 1977).
51. F. Beitia, F. Castao, M. N. Sanchez Rayo, and D. Husain, "Time-dependent study of the dynamics of the collision-induced intramultiplet mixing of $Ca(4s4p(^3P_J))$ by helium at 750 K following pulsed dye-laser generation of $Ca(4s4p(^3P_1))$," Chem. Phys. **166**, 275–285 (1992).
52. M. F. H. Schuurmans, "Superfluorescence and amplified spontaneous emission in an inhomogeneously broadened medium," Opt. Commun. **34**, 185–189 (1980).
53. R. Bonifacio, J. D. Farina, and L. M. Narducci, "Transverse effects in superfluorescence," Opt. Commun. **31**, 377–382 (1979).